Molecular-dynamics simulation of amorphous alloys. II. Self-diffusion

1989 J. Phys.: Condens. Matter 1 10003

(http://iopscience.iop.org/0953-8984/1/50/003)

J. Phys.: Condens. Matter **1** (1989) 10003–10014. Printed in the UK

Molecular-dynamics simulation of amorphous alloys: II. Self-diffusion

E H Brandt

Max-Planck-Institut für Metallforschung, Institute für Physik, D-7000 Stuttgart 80, Federal Republic of Germany

Received 10 October 1988, in final form 25 April 1989

Abstract. The self-diffusion of atoms in amorphous two-component alloys is simulated by molecular dynamics. Plots of the atomic paths show that at high temperatures T the atoms perform random walks and at low T they oscillate and eventually jump to new positions. The distribution of the atomic displacements is Gaussian with a mean square increasing at large times t as $A + 6Dt$ where A originates from oscillations and D defines the diffusion coefficient. In all amorphous systems and at the relatively high temperatures investigated $D(T)$ exhibits Arrhenius behaviour over at least three decades. The corresponding pre-exponential factors D_0 and the activation energies E are listed for various atomic interactions and masses. In all cases D_0 is 2 to 10 times $d(U/m)^{1/2}$ and E is 1.5 to 3 times U (d = position and U = depth of the minimum in the interaction potential between the majority atoms of mass m). In a given alloy the E values of small and large atoms are nearly equal and D_0 is larger for small and light atoms. Only minority atoms of very small radius exhibit markedly larger E than the majority atoms.

1. Introduction

In a previous paper (part I, Brandt 1989) amorphous arrangements of atoms are investigated which were fully relaxed by simulated annealing. The system consists of $N_A \leqslant 1000$ majority atoms and $N_B \leqslant N_A/5$ minority atoms of radii r_A and r_B and masses m_A and m_B. We use periodic boundary conditions and isotropic pair interactions between the atoms $\phi_{AA}(r)$, $\phi_{AB}(r)$ and $\phi_{BB}(r)$, which we choose as simple parabolae defined by equation (1) of part I. ϕ_{AA} and ϕ_{AB} exhibit a repulsive core and an attractive tail and are characterised by the depths (a_{AA}, a_{AB}) and positions ($d_{AA} = 2r_A$, $d_{AB} = r_A + r_B$) of their minima and by their ranges or cut-off radii (R_{AA}, R_{AB}). The interaction between the minority atoms ϕ_{BB} (with parameters a_{BB}, d_{BB}, and R_{BB}) is chosen to be merely repulsive to provide good separation between these atoms.

During the relaxation of the atomic positions the volume was kept constant or was relaxed (pressure-free relaxation). Relaxation under pressure leads to very homogeneous amorphous systems when merely repulsive smooth potentials are used (Brandt 1984, 1985, Brandt and Kronmüller 1987).

In the present paper (part II) the self-diffusion of the atoms in these amorphous systems is investigated with the aim of getting some insight into possible diffusion mechanisms as discussed, for example, by Kronmüller and Frank (1989). We use the same molecular-dynamics method as for the relaxation by annealing in part I but now

0953-8984/89/5010003 + 12 $02.50

the system runs freely, i.e. the temperature is not controlled. During the time evolution of the system the potential energy U_{pot} and the kinetic energy U_{kin} both fluctuate slightly. The constancy of the total energy $U_{tot} = U_{pot} + U_{kin}$ serves as a test for the accuracy of the time integration of Newton's equation for each atom for which we use the velocity form of the Verlet algorithm (Swope *et al* 1982). The temperature T is defined by the time average $\langle U_{kin} \rangle = \frac{3}{2} kTN$ (equipartition principle, $N = N_A + N_B$).

The temperature-dependent diffusion coefficient is calculated in the following way. We start with the system far from static equilibrium corresponding to a high temperature. Between subsequent runs the temperature is reduced by stopping the atoms (this roughly reduces T to $T/2$) or by reducing their velocity by a constant factor. After this slowing down the atoms start to move again. After 50 to 100 time steps dynamic equilibrium is reached again. Now we put $t = 0$ and store the atomic positions as references. From then on the mean-square atomic displacement at large t increases as

$$\delta^2 \equiv \langle (\Delta \boldsymbol{r}_i)^2 \rangle_i = A + 6Dt + \text{fluctuations}. \tag{1}$$

Here the constant term originates from oscillating atoms and the linear term from three-dimensional diffusive motion. Equation (1) defines the diffusivity D. Partial diffusivities D_A and D_B are defined by averaging in (1) over the A-type or B-type atoms, respectively.

As energy unit we chose U_A, as length unit d_{AA} and as mass unit m_A. $U_A = a_{AA}$ is the depth and $d_{AA} = 2r_A$ the position of the minimum in the interaction of the majority atoms of mass m_A. From these units follow the units for time and diffusion coefficient:

$$\begin{aligned} \hat{t} &= 2r_A(m_A/U_A)^{1/2} \\ \hat{D} &= 2r_A(U_A/m_A)^{1/2}. \end{aligned} \tag{2}$$

Dimensionless measures for the temperature are kT/U_A or, preferably, the ratio $\tilde{T}$ of the average kinetic energy and the equilibrium potential energy $U_{pot}^0 = -NU_B$. Here U_B is the binding energy per atom in our model system.

For atoms interacting only with their 12 nearest neighbours (e.g. in the FCC lattice) one has $U_B = 6U_A$ and for our amorphous systems $U_B \simeq 6U_A$. We may thus define a reduced temperature

$$\tilde{T} \equiv kT/4U_A \simeq \langle U_{kin} \rangle / NU_B. \tag{3}$$

The paper proceeds as follows. After this introduction, atomic paths are presented in § 2 in order to visualise the atomic motion at various temperatures. The diffusive type of this motion is discussed in § 3. Arrhenius plots of the diffusivities are given in § 4. Quantitative results for the temperature-dependent diffusivities are compiled in table 1 and discussed in § 5 for model systems with various composition and atomic interaction. Finally, the results are summarised and discussed in § 6.

2. Diffusion paths

A major problem in plotting the motion of atoms is to find an appropriate presentation. While part I dealt with the visualisation of three-dimensional static arrangements of atoms, now an additional variable, time, has to be presented. The following plots show the paths of individual atoms but not their surroundings, which, of course, are also in motion. This presentation is a first step towards a more instructive (but possibly confusing) simultaneous presentation of the paths of several neighbouring atoms that move in a correlated way.

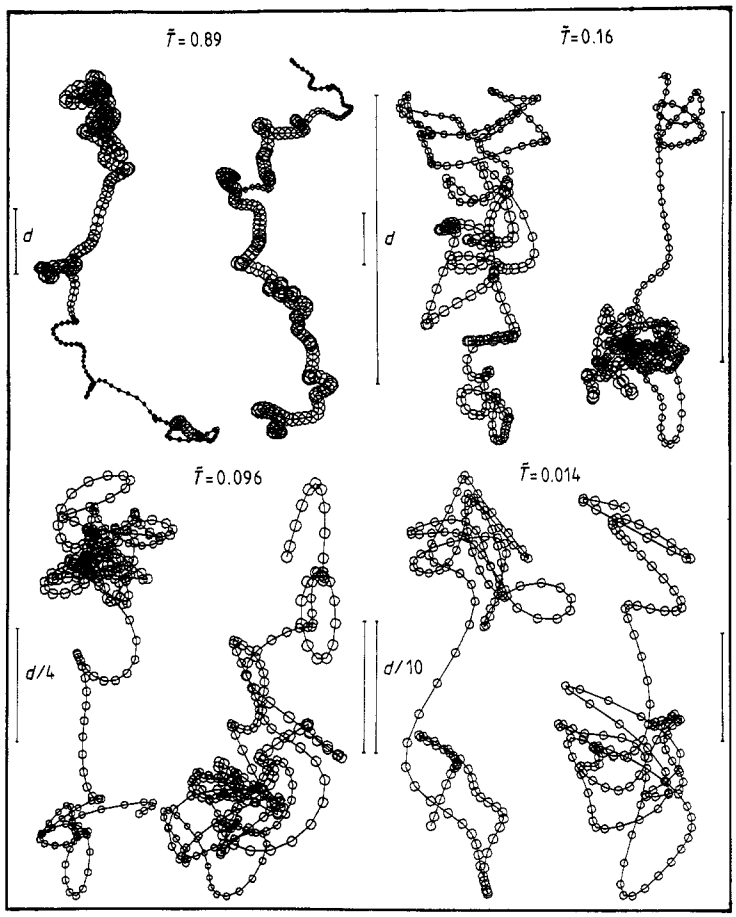

Figure 1. The atomic paths in an amorphous system at four reduced temperatures $\tilde{T}$, equation (3). The position of one atom at equidistant time intervals is marked by small octagons, the diameter of which is a measure of the coordinate perpendicular to the plane of the figure. The length scale is given in units of the closest-packed atomic distance, d. See text.

Each of the following figures shows the two longest atomic paths of a given computer run. Most of the remaining atoms moved considerably less far. Every second time step we store all atomic positions and at the end of this run pick out those atoms which have moved farthest in the xy-plane. For better resolution each path $\{x(t), y(t)\}$ is then plotted to full scale; the length scales of the paths are indicated at the right and left borders of the plots ($d = d_{AA}$). The third coordinate $z(t)$ is visualised by the size of the plotted octagons.

Figure 1 shows atomic paths for the same amorphous system at various temperatures $\tilde{T} = 0.89$ to $\tilde{T} = 0.014$. This system consists of $N_A = 200$ atoms of one type ($N_B = 0$) with interaction range $R_{AA} = 1.3$. The individual diffusion paths of the small and large atoms in alloys or in larger systems look similar to the paths depicted here and are thus not shown in this paper. Roughly 12 time intervals (the distance of the octagons) of duration $2\Delta t = 0.012$ correspond to one oscillation period $\tau \simeq 12 \times 2\Delta t = 0.144$ as can be seen at $\tilde{T} = 0.014$. Each path has a total duration of $261 \times 2\Delta t = 3.1 \simeq 22\tau$ ($\tilde{T} > 0.014$) or

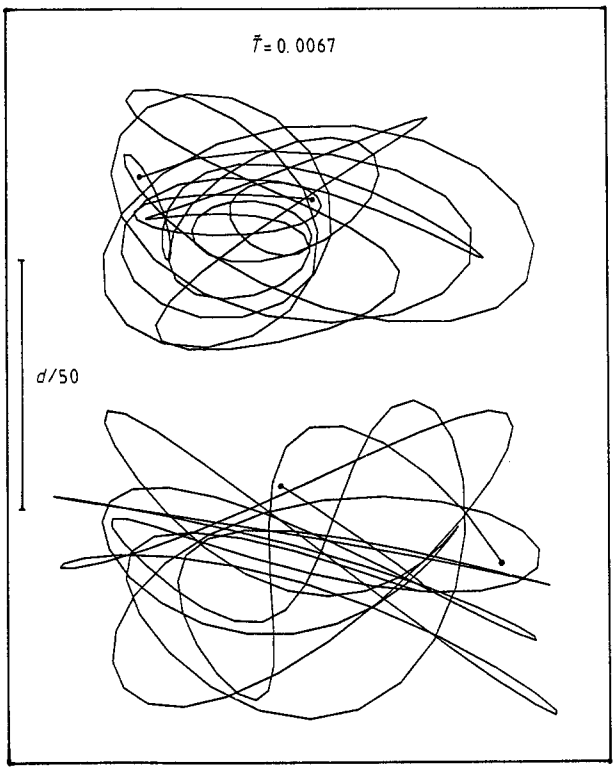

Figure 2. Atomic paths of two atoms in an FCC lattice at very low temperature. The paths in our amorphous models look very similar. See text.

$151 \times 2\Delta t = 1.8 \simeq 13\tau$ ($\tilde{T} = 0.014$). The total displacement (separation of the path ends) ranges from $s/d = 7.3$ at $\tilde{T} = 0.89$ to $s/d = 0.16$ at $\tilde{T} = 0.14$.

At higher temperatures close to the melting point ($\tilde{T} = 0.89$) the atomic paths are much longer than the atomic spacing ($\simeq d$) and look like random walks. When the temperature is lowered ($\tilde{T} = 0.16$) the atoms spend more time at energetically favourable positions roughly one atomic spacing apart. Here they orbit and oscillate irregularly and then move or jump with nearly constant speed to the next position. The number of oscillations performed at these sites increases with decreasing temperature. At still lower temperature ($\tilde{T} = 0.014$) the paths resemble rather irregular Lissajous figures with eventual jumps by less than one atomic spacing.

At very low temperatures the Lissajous figures become more regular and look similar to those in crystalline systems. This is shown in figure 2 for an ideal FCC lattice of 108 atoms at $\tilde{T} = 0.0067$ for $R_{AA} = 1.3$ ($2\Delta t = 0.008$, 202 plotted points, total time interval $202 \times 2\Delta t = 1.62$, amplitude of oscillations $\simeq 0.04d$ and period $\tau \simeq 18 \times 2\Delta t = 0.144$ as in figure 1 at $\tilde{T} = 0.144$). At that low temperature atomic jumps occur, and diffusive motion can be detected only after a prohibitively long simulation time or in extremely large systems.

For the computation of diffusivities at low temperatures, therefore, direct molecular dynamics cannot be used since it describes too small systems at too short physical time. Small diffusivities may be calculated by less direct simulation methods based on some model. For example, Lançon *et al* (1985) describe self-diffusion as a random walk of interstitial atoms through an amorphous structure, which they investigate by a Monte Carlo technique.

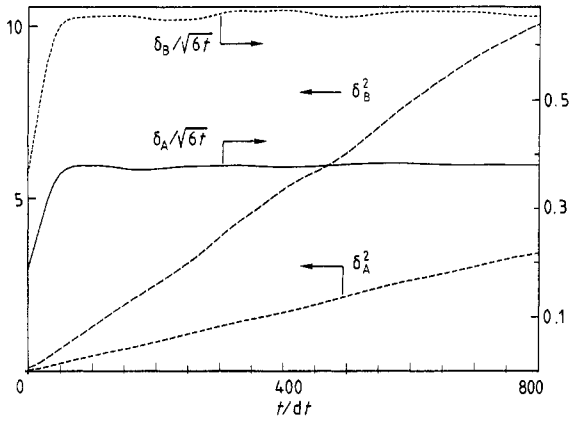

Figure 3. Mean-square displacements δ_A and δ_B of the atoms in an alloy $A_{80}B_{20}$ with the B-type atoms half as large as the A-type atoms; see text. Also shown are the ratios $\delta/\sqrt{6t}$, which tend to the constant values $\sqrt{D_A}$ and $\sqrt{D_B}$ at large times. The abscissa gives the number of time steps. High reduced temperature $\tilde{T} = 0.165$.

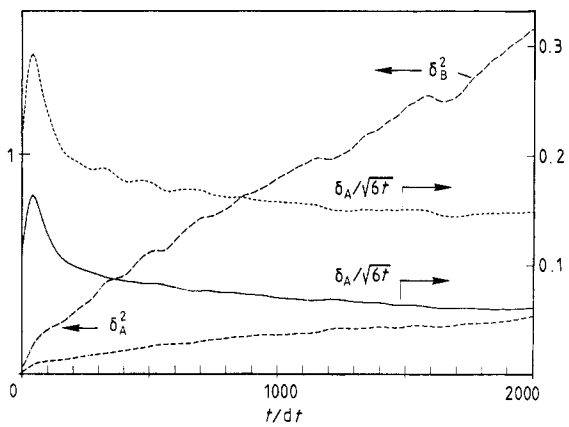

Figure 4. As figure 3 but for lower reduced temperature $\tilde{T} = 0.069$.

3. Diffusive motion

Figures 3 and 4 show the mean-square atomic displacements δ_A^2 and δ_B^2 of large (A-type) and small (B-type) atoms as a function of time t ($N_A = 800$, $N_B = 200$, $d_{AB} = 0.75$, $a_{AB} = 1$, $R_{AB} = 1.25$, $R_{AA} = 1.4$, $d_{BB} = 1$, $a_{BB} = 0.5$, $R_{BB} = 1.4$, $m_B = 0.25$; cf. the runs in figure 6(b) and D1 in table 1). The linear increase indicates the diffusive character of the motion; cf. equation (1). Also shown are the ratios $\delta_A/(6t)^{1/2}$ and $\delta_B/(6t)^{1/2}$, which tend to the constant values $\sqrt{D_A}$ and $\sqrt{D_B}$ at larger times. In figure 3 the temperature is high, $\tilde{T} = 0.165$; δ_A^2 and δ_B^2 are almost proportional to t since the contributions of both the atomic oscillations and the statistical fluctuations are very small. At the end of this run (after 800 time steps of length $\Delta t = 0.004$, $t_{max} = 3.84$) the large (small) atoms have moved an average distance of $\delta_A = 1.82$ ($\delta_B = 3.15$) atomic spacings d.

In figure 4 the temperature is lower, $\tilde{T} = 0.069$, and δ_A^2 and δ_B^2 fluctuate randomly about their ideal, slightly curved values. After 2000 time steps of length $\Delta t = 0.006$ ($t_{max} = 12$) the atoms on average have moved only small distances $\delta_A = 0.52$ and $\delta_B = 1.25$ atomic spacings. The sums of the squared displacements, $N_A\delta_A^2 = 216$ and $N_B\delta_B^2 = 312$, however, are still sufficiently large to yield significant diffusivities (statistical error $\simeq 10\%$ in this case; cf. the data points with the lowest D value in figure 6(b)).

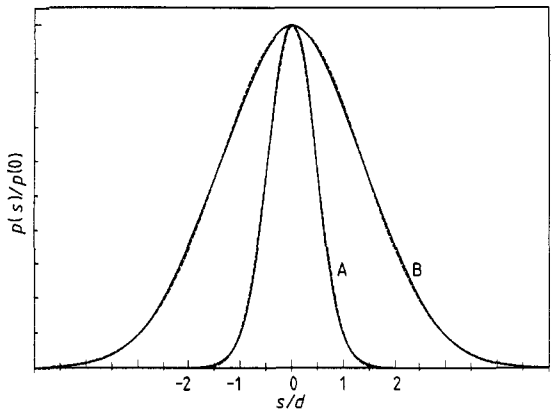

Figure 5. The distribution $p(s)$ of the atomic displacements; see text. Curve A, $\tilde{T} = 0.46$, $\delta/d = 1.65$; curve B, $\tilde{T} = 0.20$, $\delta/d = 0.56$. The broken curves (practically coincident with the full curves) are Gaussians of the same width as $p(s)$.

The diffusivities in figures 6, 7 and 8 and in table 1 below are obtained by fitting straight lines to $\delta_A^2(t)$ and $\delta_B^2(t)$ in the interval $0.4 \leq t/t_{max} \leq 1$.

A further indication of the diffusive motion is the distribution $p(s)$ of the atomic displacements. We define $p(s)$ as the probability that s_x, s_y or s_z equals s or $-s$. This choice reduces the statistical fluctuation of $p(s)$ by a factor of $\sqrt{6}$ as compared to the probability to find, e.g., $s = s_x$. Figure 5 shows two such distributions for a system of $N_A = 1000$ atoms ($N_B = 0, R_{AA} = 1.3$) at two temperatures $\tilde{T} = 0.46$ and $\tilde{T} = 0.20$. After 500 time steps of length $dt = 0.006$ the root-mean-square diffusion path along a given direction is $\delta \equiv \langle s^2 \rangle^{1/2} = 1.65d$ and $\delta = 0.56d$. The broken curves are Gaussians $\exp(-s^2/2\delta^2)$ of the same width as $p(s)$. The depicted $p(s)$ (smoothened by convolution with a Gaussian of width $\ll\delta$) practically coincide with the Gaussians at both temperatures. This is expected for diffusive motion.

4. Temperature dependence of diffusion coefficients

Arrhenius plots of the diffusivities of the A-type and B-type atoms are presented in figures 6 to 8 for systems with $N_A = 800$ and $N_B = 200$. The corresponding pre-exponential factors D_A^0 and D_B^0 and the activation energies E_A and E_B of ideal Arrhenius behaviour,

$$D_A(T) = D_A^0 \exp(-E_A/kT) \qquad D_B(T) = D_B^0 \exp(-E_B/kT) \tag{4}$$

obtained by fitting straight lines to the data points in figures 6 to 8 and other such plots, are presented in table 1. Figure 6 compiles the results of two separate runs (with different starting configurations) each for six temperatures, and this for three systems. The systems in figures 6(a) and (c) differ only by one parameter from that in figure 6(b) which exhibits $R_{AA} = 1.4$, $d_{AB} = 0.75$, $R_{AB} = 1.25$, $a_{AB} = 1$, $d_{BB} = 1$, $R_{BB} = 1.4$, $a_{BB} = 0.5$, $m_B = 0.25$, volume = constant (cf. run D1 in table 1). This system exhibits $D_B \simeq 2.7D_A$ at all temperatures depicted here ($E_A \simeq E_B$).

In figure 6(a) the interaction ϕ_{AB} is stronger by a factor of 2 ($a_{AB} = 2$, cf. run D2 in table 1). As expected, this decreases the diffusivity of the (now stronger bound) B-type atoms, $D_B \simeq 1.4D_A$ at all temperatures. In figure 6(c) the B-type atoms are four times heavier ($m_B = 1$, cf., run D4 in table 1). This again reduces D_B but now the reduction is larger at higher temperatures ($E_B < E_A$).

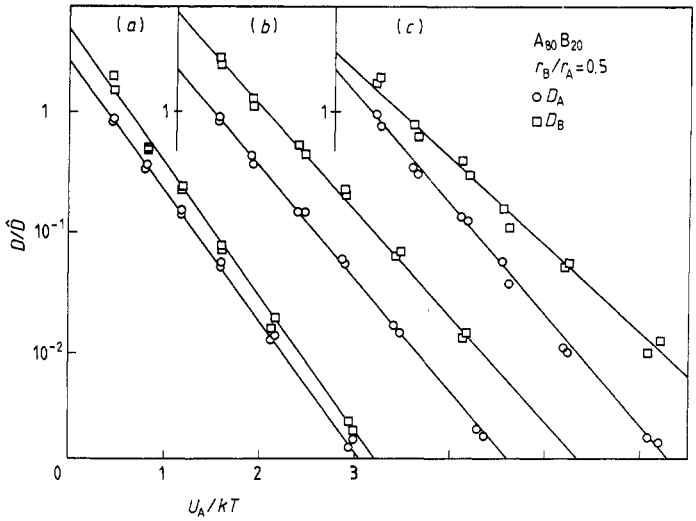

Figure 6. Arrhenius plots of the self-diffusion coefficients for three amorphous model alloys differing by only one parameter; see text. Note the shift of the origins of the abscissae and the rather small scatter of data points resulting from two equivalent runs. Within this statistical error the partial diffusivities D_A and D_B fall on straight lines in the depicted temperature interval. The unit $\hat{D}$ is defined in equation (2).

In the three systems shown in figure 6 the diffusivities obey almost ideal Arrhenius laws over the depicted temperature range (1:7) and over almost three orders of magnitude of D. Furthermore, we find nearly the same slope for both D_A and D_B. Only very small B-type atoms exhibit clearly smaller activation energy. This is shown in figure 7 for $r_B/r_A = 0.2$ (run B3 in table 1). In this case one has $E_B/E_A = 0.57$; cf. the discussion below of table 1. A case of large minority atoms is shown in figure 8 for $r_B/r_A = 1.6$ (run E6 in table 1). As expected the larger atoms diffuse more slowly. The slopes of the Arrhenius lines are nearly equal, $E_B/E_A = 1.11$. Figure 8 compiles the results of three independent runs with different starting configurations.

In the case shown in figure 8 the simulation was extended to very high temperautres, $\tilde{T} = 1.73$, where we expect the system to be liquid. At such high temperatures, with increasing T the diffusivities increase faster than expected from the extrapolation of the Arrhenius line. In particular one may have $D(T) \gg D_0$. The deviation from an Arrhenius behaviour occurs when kT becomes comparable to or larger than the activation energies E_A or E_B. It probably indicates a change in the diffusion mechanism. A similar deviation, with $D(T) \sim T^2$ at larger T, was observed in liquid tin and liquid tin–indium alloys in Spacelab experiments (Frohberg 1988, Frohberg *et al* 1987). There, the enhanced diffusivity was explained by the presence of vortex-like modes of atomic motion excited at high temperatures and contributing to the self-diffusion coefficient in the liquid metal. Very large systems, are required to simulate this type of diffusion quantitatively on a computer. For a review of self-diffusion in liquid metals and alloys, see Nachtrieb (1976).

We thus cannot at present give an explanation for the deviation from the Arrhenius line in figure 8. Possibly this indicates the existence of a spectrum of (effective) activation energies, with the large values determining the self-diffusion at large temperatures. Also we cannot exclude the possibility that, if we could extend our simulation to lower

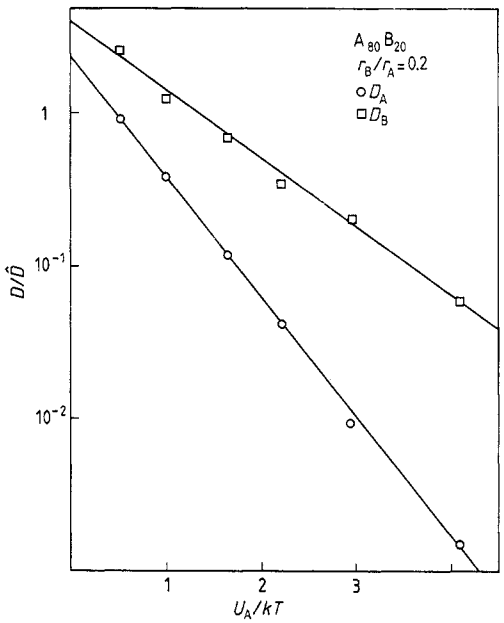

Figure 7. Arrhenius plots of the self-diffusion coefficients in an amorphous alloy with very small minority atoms. In the depicted temperature interval both D_A and D_B fall on straight lines but now with clearly different slope.

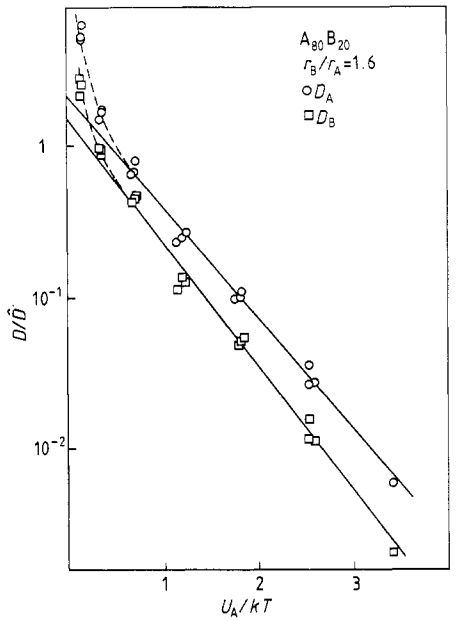

Figure 8. Arrhenius plot for an amorphous alloy with large minority atoms. Note the deviation from the Arrhenius line at very high temperatures; see text.

temperatures, the Arrhenius plots would exhibit a curvature because the effective activation energy differs at low temperatures. The computational effort required to check this would be larger by at least two orders of magnitude than that of the present paper. The present simulations show that for a wide variety of amorphous systems $D(T)$ exhibits Arrhenius behaviour with constant activation energy over at least three orders of magnitude in D and a temperature range of 1:7, which probably begins above the melting temperature. At present we do not know the melting temperature of our systems but intend to get more information on this by measuring the viscosity in future computer runs, e.g., by the method used by Chen *et al* (1988).

5. Quantitative results

Table 1 compiles the activation energies E_A and E_B (in units U_A) and the pre-exponential factors D_A^0 and D_B^0 (in units $\hat{D}$, equation (2)) of various amorphous systems. Each entry is obtained by fitting an Arrhenius line to the diffusivities resulting from at least six computer runs at various temperatures. The longest run (lowest temperature) typically needed a CPU time of one hour on a BASF 778 computer. All presented results are reproducible and independent of the (random) starting configuration of atoms.

All the systems in table 1 contain $N = 1000$ atoms. Case A contains only one type of atom ($N_B = 0$); cases B, C and D contain $N_B = 200$ smaller atoms; and case E contains $N_B = 200$ larger atoms. The table lists as input parameters the range R_{AA}, width d_{AB},

Table 1.

Name of run	R_{AA}	d_{AB}	a_{AB}	a_{BB}	m_B	Volume	E_A	E_B	D_A^0	D_B^0
A1	1.3	—	—	—	—	c	3.28	—	12.18	—
A2	1.4	—	—	—	—	c	2.20	—	1.80	—
A3	1.4	—	—	—	—	r	2.61	—	7.62	—
B1	1.4	0.6	0.25	0.5	0.25	c	1.82	0.58	2.23	3.53
B2	1.4	0.6	0.5	0.5	0.25	c	2.00	0.74	2.83	3.13
B3	1.4	0.6	1	0.5	0.25	c	2.00	1.14	2.36	4.06
B4	1.4	0.6	2	0.5	0.25	c	2.24	1.92	2.89	3.90
B5	1.4	0.6	1	0.5	1	c	1.92	2.28	2.14	3.13
C1	1.3	0.75	1	0.5	0.25	c	2.10	1.92	6.82	14.9
C2	1.3	0.75	2	0.5	0.25	c	2.56	2.37	1.43	3.13
C3	1.3	0.75	2	0.5	0.25	r	3.46	3.00	5.47	5.49
C4	1.3	0.75	2	0.5	1	c	2.27	2.25	0.85	1.46
C5	1.3	0.75	1	0.5	0.25	r	3.00	2.46	5.70	9.39
C6	1.3	0.75	1	0.5	4	r	3.31	3.30	4.06	4.95
D1	1.4	0.75	1	0.5	0.25	c	1.90	1.70	2.32	6.17
D2	1.4	0.75	2	0.5	0.25	c	2.13	2.10	2.56	3.67
D3	1.4	0.75	2	0.5	0.25	r	2.45	2.32	2.23	3.13
D4	1.4	0.75	1	0.5	1	c	1.92	1.47	2.23	3.19
E1	1.5	1.3	1	1	1	r	2.19	2.20	4.95	3.53
E2	1.5	1.3	2	1	1	r	3.36	3.86	6.30	4.22
E3	1.5	1.3	2	2	1	r	4.19	4.50	11.9	7.10
E4	1.5	1.3	1	0.5	1	r	1.70	1.72	2.66	2.01
E5	1.5	1.3	1	2	2	r	2.20	2.20	5.47	3.06
E6	1.5	1.3	1	2	1	r	1.84	2.05	3.19	2.23

and amplitudes a_{AB} and a_{BB} of the interaction potentials (cf. equation (1) of part I) and the mass m_B of the minority atoms. The remaining input parameters are $d_{AA} = a_{AA} = m_A = 1$ and, for $R_{AA} = 1.3\,(1.4, 1.5)$: $R_{AB} = 1.15\,(1.25, 1.8)$, $d_{BB} = 1\,(1, 1.2)$ and $R_{BB} = 1.3\,(1.4, 1.8)$. The types of the potentials are (cf. equation (1) of part I) $\phi_{AA} = \phi_2$, $\phi_{AB} = \phi_2$ (but $\phi_{AB} = \phi_3$ when $d_{AB} = 0.6$), and $\phi_{BB} = \phi_1$. The table also indicates whether the volume was kept constant (c) or relaxed (r).

We discuss the results of table 1 by comparing pairs of runs which differ only in one parameter. From the one-component systems A1/A2 one sees that the softer potential ($R_{AA} = 1.4$ in A2) yields smaller $D_0 = D_A^0$ but also smaller $E = E_A$ than the harder potential ($R_{AA} = 1.3$ in A1). The Arrhenius lines thus cross at a (rather high) temperature $kT \simeq 0.56U_A$. When the volume is allowed to relax (case A3) the activation energy increases as compared to the cases with constant volume (kept at the closest-packed value, case A2). This may be explained by the increase of the volume at higher T, which reduces the atomic interaction and thus enhances $D(T)$. Within the accuracy of our simulation this expansion effect is fitted by an enhanced effective activation energy.

The systems C1 to D4 contain small minority atoms with $d_{AB} = 0.75$ ($r_B/r_A = 0.5$, cf. figure 6) with harder ($R_{AA} = 1.3$, C1 to C6) and softer ($R_{AA} = 1.4$, D1 to D4) inter-

actions. As expected, the activation energy of the smaller minority atoms is always smaller, $E_B \lesssim E_A$. However, the difference is quite small although the minority atoms are twice as small as the majority atoms. Since the prefactors are also almost equal, $D_B \gtrsim D_A$, we have the interesting result that in the considered amorphous alloys of composition $A_{80}B_{20}$ the small minority atoms do not diffuse considerably faster than the larger majority atoms. Only *very small* atoms diffuse markedly faster; this is shown in the cases B1 to B5 for $d_{AB} = 0.6$ ($r_B/r_A = 0.2$, cf. figure 7).

Finally, the systems E1 to E6 in table 1 contain *large* minority atoms with $d_{AB} = 1.3$ ($r_B/r_A = 1.6$, cf. figure 8). In this case one always finds $D_B(T) < D_A(T)$. Again, the activation energies are almost equal, $E_B \gtrsim E_A$. As expected, E_B/E_A increases when the potentials ϕ_{AB} or ϕ_{BB} are chosen stronger ($a_{AB} > 1$ or $a_{BB} > 1$, cases E2, E3 and E6). When the mass m_B is increased (cf. E5/E6) one gets again $E_B \simeq E_A$ possibly since heavy large minority atoms hinder the diffusion of the majority atoms.

In general we find that softer potentials ($R_{AA} = 1.4$) yield smaller activation energies E_A and E_B than harder potentials ($R_{AA} = 1.3$); cf. the pairs A1/A2, C1/D1, C2/D2 and C3/D3. E_B is increased and D_B^0 decreased and thus D_B reduced at all temperatures, when either the mass m_B or the interaction a_{AB} is increased or when the volume is allowed to relax.

6. Summary and discussion

In molecular-dynamics simulations of amorphous alloys at high temperatures the atoms perform random walks with no clearly visible structure. At lower temperatures the atoms oscillate and from time to time jump to new positions. At very low temperatures they perform irregular Lissajous figures and jumps cannot be observed within our limited time of computation. The motion of atoms is diffusive if monitored over a sufficiently large time: the path lengths have a Gaussian distribution, and the mean-square atomic displacement increases linearly in time with the slope $6D$ defining the self-diffusivity D of the atoms. The diffusivities obtained for various model alloys exhibit a temperature dependence of the Arrhenius type with constant activation energies over three decades of D.

The diffusion coefficients and activation energies obtained may be expressed in physical units, e.g. by interpreting the A-type atoms as Fe atoms. This choice gives $m_A = m_{Fe} = 9.27 \times 10^{-26}$ kg and $d_{AA} = 2r_A = d_{Fe} = 2.47 \times 10^{-10}$ m, the atomic distance in BCC iron. The choice of the potential depth U_A is more problematic. It is known that large values result when the potential is fitted to measured binding energies, and smaller values when the potential is constructed to reproduce the elastic constants of the metal. The physical reason for this difference is that the full interaction of atoms in a metal is not well described by a simple central interaction between mainly the nearest neighbours. In metals a large contribution to the cohesive energy comes from the electron gas, which may be accounted for approximately by fitting a density-dependent interaction potential (Finnis and Sinclair 1984, Daw and Baskes 1983, 1984).

The situation here is similar to that in the flux-line lattice in type-II superconductors. If one assumes that a central interaction between pairs of flux lines yields both their binding energy (obtainable from measured magnetisation curves) and the elastic constants of the flux-line lattice (which play an essential role in flux-line pinning; Brandt and Essmann 1987) one obtains the correct bulk modulus but a completely wrong shear modulus, which increases monotonically with increasing applied magnetic field B

(Labusch 1967). The correct shear modulus of the flux-line lattice, however, vanishes as $(B_{c2} - B)^2$ when B approaches the upper critical field B_{c2} of the superconductor (Labusch 1969, Brandt 1969, 1986). Both in atomic and flux-line lattices the interaction is to a good approximation composed of a structure-dependent part and a part depending only on the local density of atoms or flux lines.

If we take the potential constructed by Chang and Graham (1966) for BCC iron we get $U_A = 0.19$ eV and $d_{AA} = 2.684 \times 10^{-10}$ m and for the reduced units, equation (2), $\hat{t} = 4.68 \times 10^{-13}$ s and $\hat{D} = 1.54 \times 10^{-7}$ m^2 s^{-1}. Similar values result from the potentials of Johnson (1966) and of Seeger and Tichy (1989). A simulation of 2000 time steps (figure 4) thus describes only about 10^{-9} s real time of the system. The temperature scale of figures 6 to 8 follows from $U_A/k = 2205$ K; the explicit temperature interval in which self-diffusion was simulated is $0.6 \leqslant U_A/kT \leqslant 4$ corresponding to 550 K $\leqslant T \leqslant$ 3600 K. This means that at the highest temperature of the simulation our model system was liquid and at the lowest temperature of $\simeq$280 °C it was an amorphous solid below the temperature range where annealing leads to crystallisation.

The main result of the present simulation is that, for all the amorphous systems we have investigated, the pre-exponential factors and activation energies (table 1) of self-diffusion are of the order of our reduced units, equation (2). In particular, the diffusivities of small, large, light or heavy atoms in a given alloy are of the same order of magnitude, with small differences as expected (light and small atoms diffuse faster). We typically find (table 1) $E_A \simeq E_B \simeq 2.5U_A \simeq 0.5$ eV (if $U_A \simeq 0.2$ eV) and $D_A^0 \simeq D_B^0 \simeq 4\hat{D} \simeq 6 \times 10^{-7}$ m^2 s^{-1}.

These findings are in marked contrast to the experimental results of Horváth *et al* (1988) discussed by Kronmüller and Frank (1989). These radio-tracer experiments in amorphous Fe–Zr alloys of various compositions yield diffusivities of the Fe and Zr atoms which, for the same alloy and temperature, differ by several orders of magnitude, and pre-exponential factors D_0 which scatter over 14 orders of magnitude. The reason for this discrepancy between the experimental and the simulated diffusivities is not clear to us at present. On the other hand, these radio-tracer experiments (with pre-annealing) are excellent and reproducible. On the other hand, our molecular-dynamics simulations are straightforward, a mere integration of the classical equations of motion of the atoms, starting with random positions. Within this classical treatment the thermodynamics of our (small) system follows from simple averages over time and over the atoms. Additional restrictions, such as, for example, keeping the total kinetic energy (the temperature) constant by continuously rescaling the velocities, or the introduction of some local dissipation of energy would mean that we treat a specific model, which has to be justified by physical arguments.

In the present molecular-dynamics simulations the only assumption that has a model character is that of central potentials acting between pairs of atoms. It is conceivable that at least part of the discrepancy is due to this simplification. Note that the improved potentials by Finnis and Sinclair (1984) or Daw and Baskes (1983, 1984) are still central pair potentials, which, however, depend on the local atomic density or on the configuration of neighbouring atoms. In our simulations we tried various central potentials and found that with simple two-body interaction the atoms diffuse 'collectively', i.e. that both types of atoms rearrange simultaneously and, therefore, exhibit similar diffusion coefficients.

In contrast, Horváth *et al* (1988) find a much larger diffusivity of the (slightly smaller) Fe atoms in Fe–Zr alloys. For example, in amorphous $Fe_{91}Zr_9$ at $T = 600$ K they measure $D_{Fe} \simeq 1 \times 10^{-19}$ m^2 s^{-1} and $D_{Zr} \simeq 1 \times 10^{-24}$ m^2 s^{-1} $\simeq 10^{-5} D_{Fe}$. This observation means

that the Fe atoms diffuse through an essentially immobile arrangement of Zr atoms. Since the radius of Zr atoms exceeds the radius of Fe atoms by only a few per cent, the differing diffusivities indicate that the type of interaction between the Zr atoms may be qualitatively different from that of the Fe atoms with Fe or Zr. The Zr atoms are possibly bound together more rigidly by an anisotropic potential which favours a certain bond angle or configuration number. Such a potential depends on the positions of at least *three* atoms. Its numerical implication would thus increase the computational effort considerably.

Acknowledgments

I would like to thank my colleagues E Esparza, W Frank, J Horváth and H Kronmüller for helpful and stimulating discussions.

References

Brandt E H 1969 *Phys. Status Solidi* **36** 381
—— 1984 *J. Phys. F: Met. Phys.* **14** 2485
—— 1985 *Cryst. Latt. Defects Amorph. Mater.* **11** 171
—— 1986 *Phys. Rev.* B **14** 6514
—— 1989 *J. Phys.: Condens. Matter* **1** 9985
Brandt E H and Essmann U 1987 *Phys. Status Solidi* b **144** 13
Brandt E H and Kronmüller H 1987 *J. Phys. F: Met. Phys.* **17** 1291
Chang R and Graham L J 1966 *US NBS Special Publication* **287** p 53
Chen S-P, Egami T and Vitek V 1988 *Phys. Rev.* B **37** 2440
Daw M S and Baskes M I 1983 *Phys. Rev. Lett.* **50** 1285
—— 1984 *Phys. Rev.* B **29** 6443
Finnis M W and Sinclair J E 1984 *Phil. Mag.* A **50** 45
Frohberg G 1988 *Verh Dtsch. Phys. Ges.* **23** (March) M 15-1
Frohberg G, Kraatz K H and Wever H 1987 *Mater. Sci. Forum* **15–18** 529
Horváth J, Ott J, Pfahler K and Ulfert W 1988 *Mater. Sci. Eng.* **97** 409
Johnson R A 1966 *Phys. Rev.* **145** 423
Kronmüller H and Frank W 1989 *Radiation Effects and Defects in Solids* **108** 81
Labusch R 1967 *Phys. Status Solidi* **19** 715
—— 1969 *Phys. Status Solidi* **32** 439
Lançon F, Billard L, Chambron W and Chamberod A 1985 *J. Phys. F: Met. Phys.* **15** 1485
Nachtrieb N H 1976 *Ber. Bunsenges. Phys. Chem.* **80** 678
Seeger A and Tichy G 1989 to be published
Swope W C, Andersen H C, Berens P H and Wilson K R 1982 *J. Phys. Chem.* **76** 637